J Solid State Electrochem (2007) 11: 365–371
DOI 10.1007/s10008-006-0151-x

ORIGINAL PAPER

Lei Zhang

Electrochemical synthesis of self-doped polyaniline and its use to the electrooxidation of ascorbic acid

Received: 7 August 2005 / Revised: 3 April 2006 / Accepted: 5 April 2006 / Published online: 27 April 2006

Abstract Self-doped polyaniline (PAN) film on platinum electrode surface has been synthesized via electrochemical copolymerization of aniline with orthanilic acid (OAA). Fourier transform infrared, UV–Vis, and elemental analysis indicate the formation of the copolymer and that the copolymer has the structure of a head-to-tail coupling of aniline and OAA units. It was found that the internal doping of PAN with OAA can extend the electroactivity of PAN in neutral and even in alkaline media. The obtained self-doped PAN (PAN-OAA)-coated platinum electrode is shown to be a good surface for the electrooxidation of ascorbic acid (AA) in phosphate buffer solution of pH 7. The anode peak potential of AA shifts from 0.63 V at bare platinum electrode to 0.34 V at the PAN-OAA-modified platinum electrode with greatly enhanced current response. A linear calibration graph is obtained over the AA concentration range of 5–60 mM using cyclic voltammetry. Rotating disk electrode voltammetry and chronoamperometry have been employed to investigate the electrooxidation of AA. The PAN-OAA-modified platinum electrode shows good stability and reproducibility.

Keywords Self-doped polyaniline · Aniline · Electrooxidation · Orthanilic acid · Ascorbic acid

Introduction

Among conducting polymers, polyaniline (PAN) has been attracting significant interest due to its high conductivity, good redox reversibility, and stability in media and air. These properties are favorable to its applications in rechargeable batteries [1–3] and electrocatalysis [4–10]. However, the energy density and the catalytic activity of PAN are limited by pH value because PAN has little electrochemical activity at pH>4. The potential range of the electroactivity for PAN decreases with increasing pH value [11], and its redox peaks disappear in the cyclic voltammetry when pH>5. Thus, in general, the redox potential of species to be oxidized and reduced by PAN is within the potential and pH range in which PAN itself is electroactive, restricting its application in bioelectrochemistry, which normally requires a neutral pH environment. To improve the chemical and physical properties of PAN, acidic groups (normally sulfo- or carboxyl groups) were introduced into the PAN chain and to form a so-called "self-doped" PAN, which can maintain its electrochemical activity in neutral or even basic solutions [12–17]. In this case, the inserted ionogenic groups change the microenvironment of the nitrogen atoms in the PAN chain, thus shifting the local pH. Very recently, Tian et al. [18] reported that doping PAN with COO^--modified gold nanoparticles by forming stable layer-by-layer multilayer films can shift its electroactivity to neutral pH. Xiao et al. [19] reported the bioelectrocatalytic synthesis of PAN on double-stranded DNA templates and found that the obtained PAN-DNA hybrid system was also redox active in neutral medium.

The discovery of PAN processibility simplified the procedure of preparing PAN-based films via dissolving chemically synthesized PAN in a variety of organic solvents by using organic sulfonic acids as dopants [20, 21]. Also, Lukachova et al. [22] and Karyakin et al. [6] mixed camphorsulfonic acid (CSA) with regular chemically synthesized PAN and dissolved the mixture in chloroform. The results showed that the PAN doped with CSA remained electroactive and was conducting up to pH 9.

On the other hand, a considerable effort has been devoted to the development of voltammetric methods for the determination of ascorbic acid (AA) in biological systems for many years. Ascorbic acid is a vital component in the diet of human, and it is known to take part in several biological reactions [23]. Recent clinical studies have demonstrated that the content of ascorbic acid in biological fluids can be used to assess the amount of oxidation stress in human metabolism [24], and excessive oxidative stress

L. Zhang (✉)
Department of Chemistry,
College of Life and Environment Science,
Shanghai Normal University,
Shanghai 200234, People's Republic of China
e-mail: chemzl@shnu.edu.cn

has been linked to cancer, diabetes mellitus, and hepatic disease. However, it is almost too difficult to determine this component electrochemically by direct oxidation on a conventional electrode because of its high overpotential and thus electrode fouling, poor reproducibility, low selectivity, and poor sensitivity. Thus, much interest has been focused on the use of mediators and modified electrodes to undergo catalysis the electrochemical oxidation of ascorbic acid. For example, electrode surfaces modified with immobilized quinone groups [25], adsorbed 7,7,8,8-tetracyanoquinodimethane [26], deposited nickel pentacyanonitrosylferrate [27], covalently attached amino acids [28, 29], functionalized self-assembled monolayer of 4-aminothiophenol [30], electropolymerized films of polypyrrole [31, 32], and self-doped PAN [8, 33] have all been employed via the mediator oxidation.

In this work, I present the synthesis of self-doped PAN via electrochemical copolymerization of aniline with orthanilic acid (OAA), the electroactivity of the synthesized self-doped PAN, and its electrocatalytic oxidation effect towards ascorbic acid at pH 7. The results show that copolymerization of OAA and PAN happens and ensures the self-doped PAN to be electroactive up to pH 9. In the media of 0.1 M phosphate buffer solution (PBS, pH 7), the PAN-OAA film-coated platinum electrode shows excellent electrochemical activity towards AA, reducing the oxidation potential by 0.29 V with greatly enhanced oxidation peak current. The diffusion coefficient of AA and rate constant for the electrooxidation reaction are evaluated with different electrochemical techniques.

Experimental

Apparatus

All electrochemical experiments were performed using a computer-controlled CHI 660A (CHI, USA) electrochemical analyzer in a conventional three-electrode electrochemical cell using platinum wire (f=1.5 mm) as the working electrode, twisted platinum wire as the auxiliary electrode, and Ag/AgCl (saturated KCl) as the reference electrode.

Fourier transform infrared (FT-IR) spectra were recorded on a KBr disk containing about 1 % sample by weight using a Nicolet 520 (Nicolet, USA) spectrophotometer. For each sample, a total of 120 scans at a resolution of 4 cm^{-1} was used. UV–Visible absorption spectra (UV–Vis) were performed on a Cary 500 UV–Vis-NIR spectrophotometer (Varian, USA) using 1 cm light path quartz cuvette.

Chemicals and solutions

Aniline (99.5 %, Beijing Chemical Reagent Company) was distilled under vacuum before use and stored under highly purified nitrogen. OAA was purchased from Sigma and used as received. L-ascorbic acid purchased from Fluka was used without further purification. All other chemicals used in this investigation were of analytical grade.

Ascorbic acid solution was prepared with 0.1 M PBS (pH 7) immediately before use. Sulfuric acid solutions (pH 1–3), 0.1 M acetate (pH 4–5), 0.1 M PBS (pH 6–8), and 0.1 M borate (pH 9) buffers were employed for the electrochemical investigation. All solutions were prepared using doubly distilled water purified with a Millipore-Q^+ system (18.3 MΩ).

All experiments were made at room temperature (≈24 °C). The solutions were thoroughly deoxygenated by bubbling highly purified nitrogen, and a nitrogen atmosphere was maintained over the solutions.

Electrode preparation

The platinum working electrodes were polished carefully with alumina powder (Buehler; 1.0, 0.5, and 0.03 μm, successively) on a soft polishing cloth (Buehler). After sonicating in absolute ethanol, then in water for 10 min successively, they were treated with cyclic scanning in the potential range of −0.2 to 1.2 V at 100 mV s^{-1} in 0.15 M H_2SO_4 until the cyclic voltammogram (CV) characteristic for a clean platinum electrode was obtained. Electrochemical copolymerization of aniline and OAA has been performed by continuous potential cycling for 30 min within the potential range of 0–1 V in a solution containing 0.1 M sulfuric acid, 0.01 M aniline, and 0.04 M OAA. After polymerization, the PAN-OAA film was firstly washed using sulfuric acid solution of pH 3 to remove unreacted aniline, and then washed thoroughly using 0.1 M PBS (pH 7). The PAN-OAA film-modified platinum electrode (PANOAA/Pt) was stored in 0.1 M PBS (pH 7) for use.

Results and discussions

Characterization of the copolymer

To investigate the structure and property of the copolymer, FT-IR, UV–Vis, and elemental analysis were employed to characterize the copolymer. Figure 1a shows the FT-IR spectra of PANOAA (curve a), and as a comparison, the FT-IR spectrum of PAN was also given in Fig. 1a (curve b). As shown in Fig. 1a, except for the features that are the characteristics of the sulfonated groups, the IR spectra of the copolymer are very similar to that of PAN. The large descending baseline in the spectral region of 4,000–2,000 cm^{-1} is often used to indicate the free-electron conduction in conducting polymers [34]. The broad peak centered at 3,450 cm^{-1} is attributed to unresolved N–H stretching mode. The peaks at 1,580 and 1,500 cm^{-1} are due to the stretching of the benzenoid and quinoid structures. A strong aromatic C–N stretching is responsible for the peaks at 1,302 cm^{-1}. In the lower frequency region, the peak at 1,143 cm^{-1} is due to the C–H in-plane deformation, which was used to evaluate the electron delocalization in polymers

[35]. Therefore, the enhanced IR absorption at this location indicates that the copolymers have good conductivity; this agrees well with the strong absorption by free electrons in the region 4,000–2,000 cm^{-1}. The absorptions at 1,050, 1,020, 709, and 620 cm^{-1} are the best confirmation for the presence of sulfonate functional groups attached to the aromatic rings [36]. The absorption maxima at 876 and 821 cm^{-1} are generally assigned to the out-of-plane bending of aromatic hydrogen in 1,4-disubstituded and 1,2,4-trisubstituted aromatic structures. This indicates that the copolymer have the head-to-tail coupling structure of OAA and aniline units. On the other hand, the peaks at 1,050 and 1,020 cm^{-1} are assigned to the aryl–S links, aromatic ring vibration having some C–S stretching characteristic.

Figure 1b shows the UV–Vis spectra of the copolymer in NMP solution (dashed line), and as a comparison, the electronic spectra of PAN in NMP (solid line) and a typical absorption of copolymer in 0.5 M KOH are also included (dotted line). It can be seen that the absorption bands of the copolymer in NMP shift to shorter wavelengths compared to those of PAN in the similar solution. The band at about 321 nm for PAN, assigned to the π–π^* transition of the benzenoid moiety and therefore corresponded to the bandgap of the polymer, shifts to about 294 nm. This hypsochromic shift, caused by the sulfonic acid groups attached on the benzene ring, indicates that the copolymers have a decreased conjugation and an increased bandgap due to their strong electron-withdrawing nature. The broad band at 604 nm, attributed to the intramolecule transition between the quinoid and benzenoid units in the PAN structure, shifts to about 571 nm for PANOAA. On the other hand, it can be noted that when the copolymer was dissolved in 0.5 M KOH solution, its absorption band has a larger blue shifted (536 nm) compared with that in NMP solution. This could be due to the better stability of the copolymer salt in the alkaline solution.

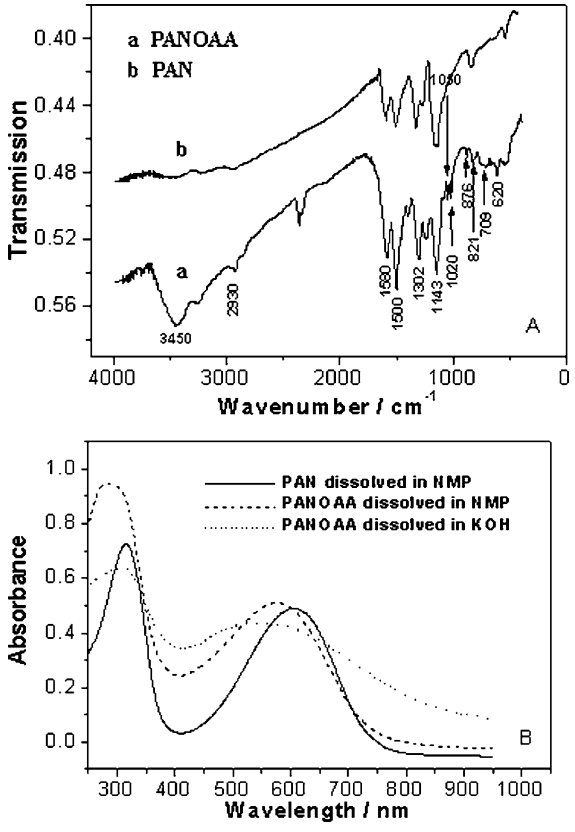

Fig. 1 **a** FT-IR spectra of PANOAA (*a*) and PAN (*b*); (**b**) UV–Vis spectra of PANOAA dissolved in NMP (*dashed line*) and in KOH (*dotted line*) and PAN in NMP (*solid line*)

To further investigate the structure of the copolymer, elemental analysis has been used to study the composition of the copolymer. The results show that when the content of OAA in reaction solution is 0.8, the fraction of OAA in the copolymer (sulfur-to-nitrogen ration S/N) is 0.42. This S/N ratio is comparable with those of the sulfonated PAN prepared by electrochemical (12~40 %) [37, 38] and chemical (15~36 %) [39] copolymerization of aniline with metanilic acid. However, it is lower than those prepared by sulfonation of the emeraldine base form (about 50 %) [40, 41] and the leucoemeraldine base (about 78 %) [42] in fuming sulfonic acid. Based on the S/N ratio, one can calculate that there should have approximately one S atom per 2.5 benzene rings in the structure of the copolymer.

Redox electroactivity of PANOAA/Pt electrode

Figure 2 shows the CVs of PANOAA/Pt electrode in various buffer solutions. As shown in Fig. 2, at pH 1, there are three pairs of redox peaks; the two sets of peaks located at around 0.1 and 0.7 V correspond to the leucoemeraldine/emeraldine and emeralding/pernigraniline transformations, respectively, and the third pair of peaks in the middle is attributed to the defects in the linear structure of the polymer [43]. At pH 3, the third pair of peaks almost disappears, and when pH≥5, the two sets of peaks overlap into one pair of peaks, which corresponds to the leucoemeraldine/pernigraniline redox reaction. This is due to the pH dependence of emeraldine/pernigraniline redox reaction. In addition, the redox activity of PAN-OAA film still remains at pH 9. The results obtained indicate the remarkable extension of the redox activity of PAN film-modified platinum electrode up to pH 9. This improvement is due to the copolymerization of aniline with organic acid dopant OAA.

Electrochemical oxidation of AA at PANOAA/Pt electrode

Cyclic voltammetry

Figure 3a shows the CVs of Pt (dashed line) and PANOAA/Pt (solid line) electrodes in AA solution, respectively. As seen in Fig. 3a, AA shows a sluggish and much smaller CV peak response with oxidation wave at about 0.63 V with an E_p–$E_{p/2}$ of 0.21 V at bare Pt electrode. Whereas, PANOAA/Pt electrode leads to an obvious negative shift of AA oxidation overpotential ($E_{p,a}$=0.34 V) and increase of the redox peak current with a more reversible behavior

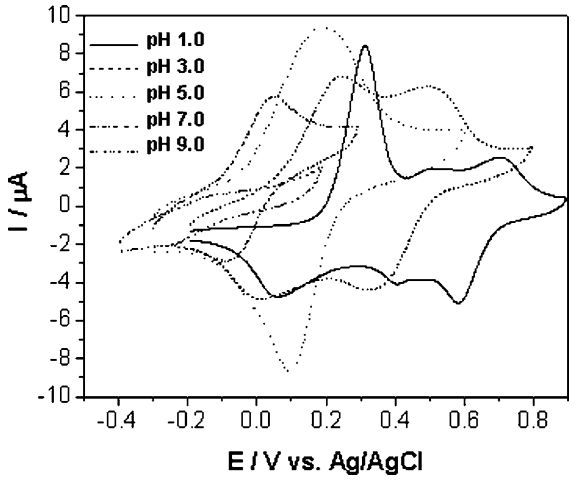

Fig. 2 Cyclic voltammograms of PANOAA/Pt electrode in different buffer solutions. Scan rate, 50 mV s^{-1}. These buffers are 0.1 M sulfuric acid (pH 1 and 3), 0.1 M acetate (pH 5), 0.1 M PBS (pH 7), and 0.1 M borate (pH 9) solutions, respectively

(E_p−$E_{p/2}$=0.10 V). The greatly enhanced peak current and the negative shifting in the anodic overpotential of 0.29 V for AA indicate the strong electrocatalytic activity of PANOAA/Pt electrode to AA. The decrease in the overpotential of AA is due to a kinetics effect, thus a substantial increase in the electron transfer rate of AA was observed, which was attributed to the improvements in the reversibility of the electron transfer processes. Figure 3b shows the CVs of different concentrations of AA at PANOAA/Pt electrode. As can be seen, the oxidation peak current increases with increasing AA concentration. The inset of Fig. 3b shows that the anode peak current is linearly dependent on the AA concentration in the range of 5–60 mM, with a correlation coefficient of 0.997.

Further investigation was made into the transport characteristics of AA in the modified electrodes. Figure 4a shows the CVs of 10 mM AA at PANOAA/Pt electrode at different scan rates. It can be seen that the catalytic effect of PAN-OAA composite film appears even at high scan rates, which is attributed to the considerable catalytic reaction rate. Also, it can be seen that the catalytic oxidation peak potential shifts to more positive with increasing scan rates, indicating a kinetics limitation in the reaction between the redox sites of PAN-OAA composite film and AA. However, the cyclic voltammetric peak currents for AA at PANOAA/Pt electrode are proportional to square root of scan rates in the range of 30–700 mV s^{-1} (inset of Fig. 4a). It indicates that the electrode reaction is controlled by diffusion process. Moreover, a plot of the scan rate-normalized current ($I/\nu^{1/2}$) vs scan rate (Fig. 4b) shows a shape typical of an electrochemical–chemical (EC) catalytic process.

Rotating disk electrode (RDE) voltammetry

The electrochemical oxidation of AA at PANOAA/Pt electrode has also been evaluated by using RDE voltammetry technique. Figure 5a shows the typical RDE responses of 5 mM AA at the PAN-OAA film-coated RDE, scanned from −0.2 to 0.8 V at 50, 100, 200, 300, 400, 700, 900, 1,600, 2,500, and 3,600 rpm with a scan rate of 5 mV s^{-1}. The current observed on the plateau (at 0.70 V) of the RDE voltammograms are used to draw Levich and Koutecky–Levich plots. If the oxidation of AA at PANOAA/Pt electrode is controlled solely by the mass-transfer process in solution, the relationship between the limiting current and rotating rate should obey the Levich equation [44]:

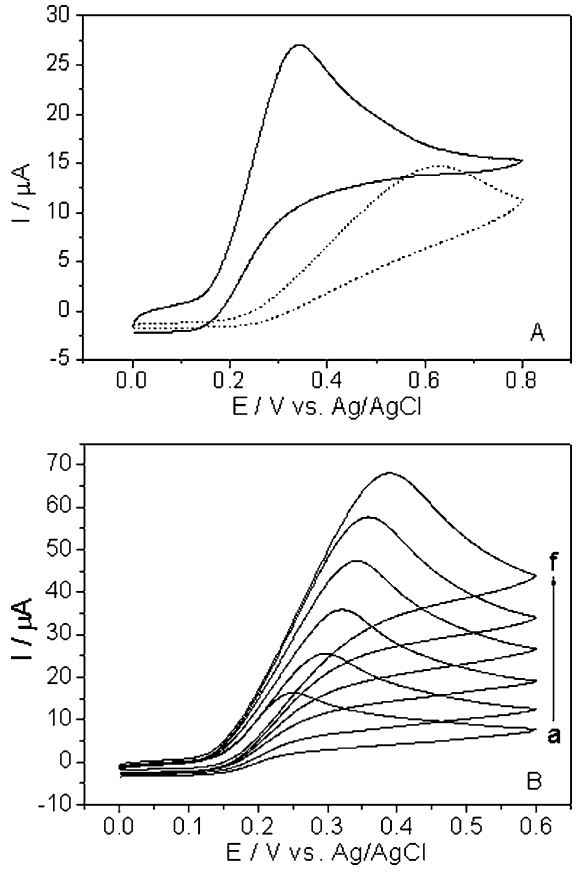

Fig. 3 **a** CVs of Pt (*dashed line*) and PANOAA/Pt (*solid line*) electrodes in 0.1 M PBS (pH 7) containing 10 mM AA. **b** CVs of PANOAA/Pt electrode in 0.1 M PBS (pH 7) containing different concentrations of AA. Concentrations of AA from (*a*) to (*f*) are 5, 15, 25, 35, 45, and 60 mM, respectively

$$I_1 = I_{Lev} = 0.620nFAD^{2/3}\nu^{-1/6}\omega^{1/2}c_0, \quad (1)$$

where D, ν, ω, and c_0 are the diffusion coefficient, the kinematic viscosity, the rotating rate, and the buck concentration of the reactant in the solution, respectively. All other parameters have their usual meanings. Based on Eq. 1, the plot of the limiting current I_l as a function of the $\omega^{1/2}$ should be a straight line intersecting the origin. Inset of Fig. 5a shows the Levich plot taken at 0.70 V for AA oxidation. The slope and intercept are found to be 1.86 μA

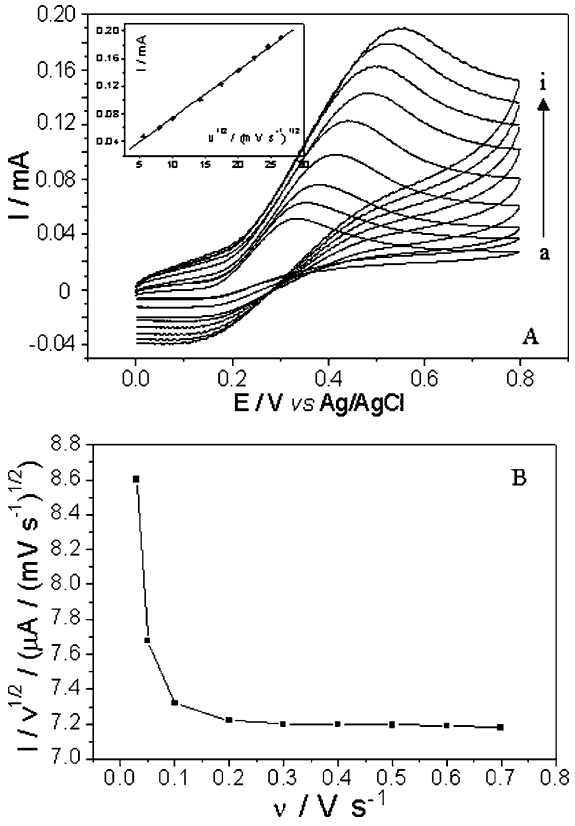

Fig. 4 **a** CVs of 10 mM AA at PANOAA/Pt electrode in 0.1 M PBS (pH 7) at different scan rates. Potential scan rates from down to up are 30, 50, 100, 200, 300, 400, 500, 600, and 700 mV s^{-1}, respectively. *Inset* shows the calibration plot of I vs $\nu^{1/2}$. **b** Plot of the anodic current function ($I/\nu^{1/2}$) vs scan rate (ν)

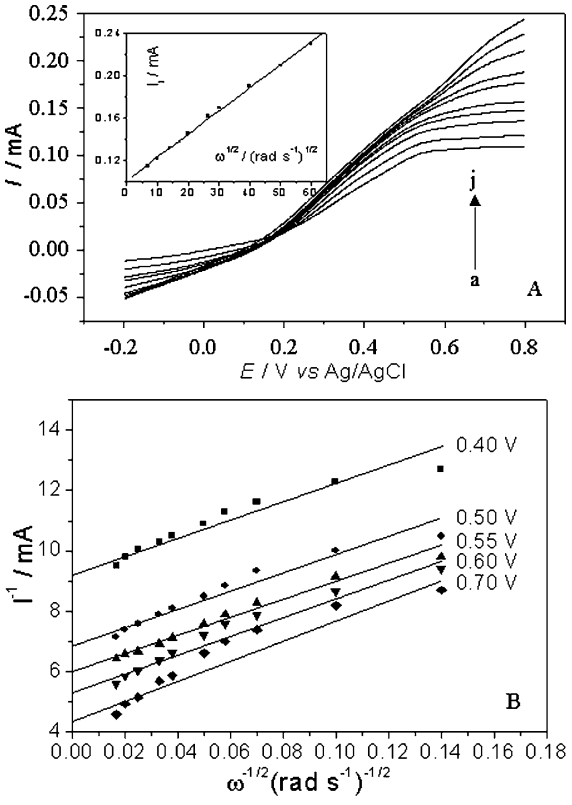

Fig. 5 **a** RDE voltammograms for the oxidation of 5 mM AA at PANOAA/Pt electrode in 0.1 M PBS (pH 7). The rotation speed from down to up are 50, 100, 200, 300, 400, 700, 900, 1,600, 2,500, and 3600 rpm, respectively, with a scan rate of 5 mV s^{-1}. *Inset* shows the Levich plot for catalytic oxidation of 5 mM AA at 0.7 V on the PANOAA/Pt electrode. **b** *K–L* plots for 5 mM AA on the PANOAA/Pt electrode at oxidation potentials of 0.40, 0.50, 0.55, 0.60, and 0.70 V, respectively

rad$^{-1/2}$ s$^{-1/2}$ and 101.5 μA, respectively. The fact that the Levich plot does not pass through the origin indicates the nonideal behavior of the PANOAA/Pt electrode, including kinetic limitation. The catalytic current I_{cat} corresponding to the mediated reaction is a function of the Levich current I_{Lev}, representing the mass transfer of AA in the solution, and the kinetic current I_k, representing the current in the absence of mass-transfer effect. Andrieux et al. [45] have described the kinetic process of the catalytic reaction at the modified electrodes and given the following equation:

$$1/I_1 = 1/I_{Lev} + 1/nFAc_0k\Gamma\left[1 - \left(I_1 d \Big/ FAc_p^0 D_e\right)\right], \tag{2}$$

where A, k, Γ, d, c_p^0, and D_e are the electrode area, the rate constant for the catalytic reaction, the surface concentration of the catalyst in the film, the film thickness, the total volume concentration of catalyst in the film, and the diffusion coefficient of electrons in the film. When the mass-transfer process in the solution and the catalytic reaction become dominant, the term $\left[1 - \left(I_1 d \Big/ FAc_p^0 D_e\right)\right]$ is essentially equal to unity and Eq. 2 reduces to the Koutecky–Levich equation [44]:

$$1/I_1 = 1/nFAc_0k\Gamma + 1/0.620nFAD^{2/3}\nu^{-1/6}\omega^{1/2}c_0 \tag{3}$$

$$I_k = nFAc_0k\Gamma. \tag{4}$$

Figure 5b shows the typical *K–L* plots for AA oxidation at PANOAA/Pt electrode measured at oxidation potentials of 0.40, 0.50, 0.55, 0.60, and 0.70 V, respectively. The I_k values can be obtained from the intercepts of the *K–L* plots. They are found to be 0.11, 0.15, 0.17, 0.19, and 0.23 mA, respectively, at these potentials. The increases of I_k with the increase of observed potentials indicate the potential-dependent kinetic behavior of the electrooxidation reaction. On the other hand, based on the value of kinematics viscosity as 1.1×10^{-2} cm^2 s^{-1} [46] and the slope of the *K–L* plot, the diffusion coefficient (D) can be obtained as 6.8×10^{-6} cm^2 s^{-1}.

Chronoamperometric measurements

Chronoamperometry has also been used to investigate the electrode process of AA at PANOAA/Pt electrode. Figure 6a shows the chronoamperometric measurements of various concentrations of AA at PANOAA/Pt electrode by setting the working electrode potential at 0.70 V. Inset of Fig. 6a shows the current responses of different concentrations of AA at fixed time of 5, 10, and 17 s, respectively. It can be seen from plots (a), (b), and (c) that the slopes of the calibrations decrease with the increasing time elapsed after potential step application. However, there is an almost similar intersection between currents measured at different time elapsed and AA concentrations. The typical *I*–*t* curve in Fig. 6a indicates that the currents observed must be controlled by AA diffusion in solution. Thus, the current corresponding to the electrochemical reaction obeys Cottrell's law [47]:

$$I = nFAD^{1/2}c_0/\pi^{1/2}t^{1/2}, \quad (5)$$

where D and c_0 are the diffusion coefficient ($cm^2\ s^{-1}$) and bulk concentration ($mol\ cm^{-3}$), respectively. Based on Eq. 5, the plot of I vs $t^{1/2}$ is a straight line, and the slope of such lines can be used to estimate the diffusion coefficient of AA. The mean value of D is found to be $6.6\times10^{-6}\ cm^2\ s^{-1}$, which is in good agreement with that obtained from the RDE technique.

Chronoamperometry can also be employed to evaluate the catalytic rate constant for the reaction between AA and the redox sites of the surface confined PAN-OAA film according to the method [48]:

$$I_{cat}/I_L = \gamma^{1/2}\left[\gamma^{1/2}\mathrm{erf}\left(\gamma^{1/2}\right) + \exp\left(-\gamma\right)/\gamma^{1/2}\right], \quad (6)$$

where I_{cat} is the catalytic current of AA at the PANOAA/Pt electrode, I_L is the limiting current in the absence of AA, and $\gamma=kc_0t$ (c_0 is the bulk concentration of AA) is the argument of the error function. When γ exceeds 2, the error function is almost equal to 1 and therefore the above equation can be reduced to:

$$I_{cat}/I_L = \gamma^{1/2}\gamma^{1/2} = \gamma^{1/2}(kc_0t)^{1/2}, \quad (7)$$

where t is the time elapsed (s). Based on the slope of the I_{cat}/I_L vs $t^{1/2}$ plot, k can be obtained for a given AA concentration. One such plot is shown in Fig. 6b constructed from the chronoamperogram of the PANOAA/Pt electrode in the absence and presence of 5 mM AA. The mean value of k in AA concentration range 5–30 mM is $6.3\times10^5\ cm^3\ mol^{-1}\ s^{-1}$.

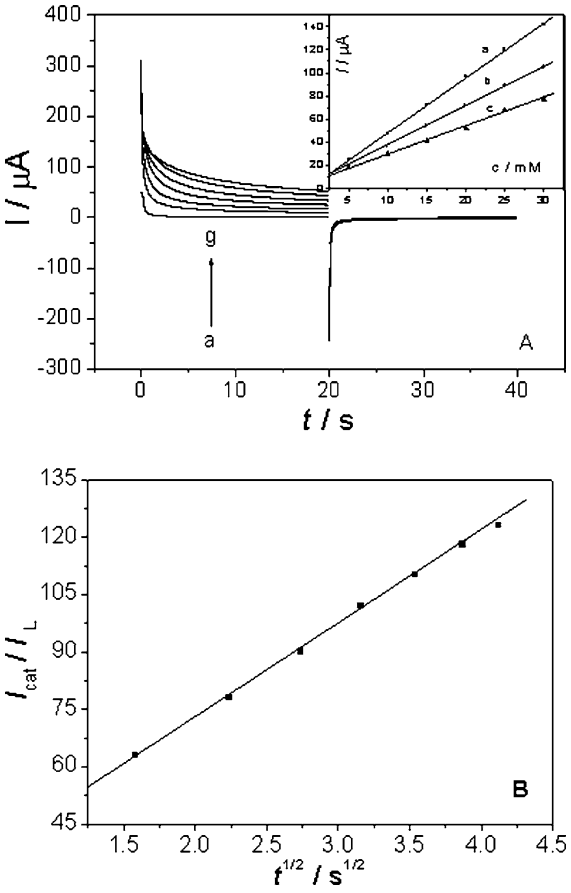

Fig. 6 Chronoamperograms obtained at PANOAA/Pt in the absence (*a*) and presence of 5 (*b*), 10 (*c*), 15 (*d*), 20 (*e*), 25 (*f*), and 30 mM (*g*) AA. The first and second potential steps are 0.7 and 0.0 V, respectively. Supporting electrolyte, 0.1 M PBS (pH 7). *Inset* shows the dependence of the fixed-time current [observed at 5 (*a*), 10 (*b*), and 17 (*c*) s after the first potential step] vs AA concentrations. **b** Dependence of I_{cat}/I_L on the $t^{1/2}$ derived from the data of chronoamperograms of (**a**) and (**b**) in Fig. 6a

Electrode stability and reproducibility

Because the procedure of electrode preparation is easy and rapid, it is not so important for the electrode to be stable for a prolonged time. However, we checked its long-term stability by measuring the response from day to day during a storage in PBS (pH 7) at 4 °C. During the first 2 days, the current response had no apparent decrease and in the next 2 weeks, the current response decreased about 11 % of its initial response, and 17 % for 1 month.

To characterize the reproducibility of the modified electrode, repetitive measurements were carried out in solutions containing 10 mM AA. The results of 10 successive measurements showed a relative standard deviation of 2.8 % for AA, indicating that the modified electrode is not subject to surface fouling by the oxidation products, which are notorious for their surface fouling effects at bare electrode.

Conclusions

This study demonstrates that the copolymerization of aniline with OAA via electrochemical procedure can extend the PAN electroactivity to neutral and even alkaline media. At pH 7 PBS, the PANOAA/Pt electrode exhibits

good electrochemical activity toward the oxidation of AA via a surface layer-mediated charge transfer. The kinetics process of the catalytic reaction can be explained by cyclic voltammetry, RDE voltammetry, and chronoamperometry. The prepared PANOAA/Pt electrode is moderately stable and can be useful for single-use devices for the practical determination of AA.

Acknowledgements I wish to acknowledge the financial support of this paper by Shanghai Leading Academic Discipline Project (T0402), Shanghai Municipal Education Commission (05DZ16), and Shanghai Normal University (PL507).

References

1. MacDiarmid AG, Mu S, Somasiri NLD, Wu W (1985) Mol Cryst Liq Cryst 121:187–190
2. Mu S, Ye J, Wang Y (1993) J Power Sources 45:153–159
3. Oyama N, Tatsuma T, Sato T, Sotomura T (1995) Nature 373:598–600
4. Kanungo M, Kumar A, Contractor AQ (2003) Anal Chem 75:5673–5679
5. Bartlett PN, Wallace ENK (2001) Phys Chem Chem Phys 3:1491–1496
6. Karyakin AA, Vuki M, Lukachove LV, Karyakina EE, Orlov AV, Karpachova GP, Wang J (1999) Anal Chem 71:2534–2540
7. Rajendra Prasad K, Munichandraiah N (2002) Anal Chem 74:5531–5537
8. Zhou D, Xu J, Chen H, Fang H (1997) Electroanalysis 9: 1185–1188
9. Mandić Z, Duić L (1996) J Electroanal Chem 403:133–141
10. Kazarinov VE, Andreev VN, Spitsyn MA, Mayorov AP (1990) Electrochim Acta 35:1459–1463
11. Huang WS, Humphrey BD, MacDiarmid AG (1986) J Chem Soc Faraday Trans 82:2385–2400
12. Wei X, Epstein AJ (1995) Synth Met 74:123–125
13. Lin HK, Chen SA (2000) Macromolecules 33:8117–8118
14. Kayakin AA, Strakhova AK, Yatsimirsky AK (1994) J Electroanal Chem 371:259–265
15. Karyakin AA, Maltsev IA, Lukachova LV (1996) J Electroanal Chem 402:217–219
16. Mažeikienė R, Niaura G, Malinauskas A (2003) Synth Met 139:89–94
17. Mu S, Kan J (2002) Synth Met 132:29–33
18. Tian S, Liu J, Zhu T, Knoll W (2003) Chem Commun 21: 2738–2739
19. Xiao Y, Kharitonov AB, Patolsky F, Weizmann Y, Willner I (2003) Chem Commun 13:1540–1541
20. Cao Y, Smith P, Heeger AJ (1992) Synth Met 48:91–97
21. Cao Y, Qiu J, Smith P (1995) Synth Met 69:187–190
22. Lukachova LV, Shkerin EA, Puganova EA, Karyakina EE, Kiseleva SG, Orlov AV, Karpacheva GP, Karyakin AA (2003) J Electroanal Chem 544:59–63
23. Martin DW Jr (1983) In: Martin DW Jr, Mayes PA, Rodwell VW (eds) Harper's review of biochemistry, 19th edn. Lange, Los Altos, CA, p 112
24. Koshiishi I, Imanari T (1997) Anal Chem 69:216–220
25. Chihiro Ueda, Daniel Chi-Sing Tse, Theodore Kuwana (1982) Anal Chem 54:850–856
26. Murthy ASN, Anita (1994) Biosens Bioelectron 9:439–444
27. Pournaghi-Azar MH, Razmi-Nerbin H (2000) J Electroanal Chem 488:17–24
28. Zhang L, Sun Y, Lin X (2001) Analyst 126:1760–1763
29. Zhang L, Lin X (2001) Analyst 126:367–370
30. Zhang L, Jia J, Zou X, Dong S (2004) Electroanalysis 16: 1416–1418
31. Mao H, Pickup PG (1989) J Electroanal Chem 265:127–142
32. Lyons MEG, Breen W, Cassidy J (1991) J Chem Soc, Faraday Trans 87:115–123
33. Xu J, Zhou D, Chen H (1998) Fresenius J Anal Chem 362:234
34. Cao Y, Li S, Xue Z, Guo D (1986) Synth Met 16:305–315
35. Chiang JC, Macdiarmid AG (1986) Synth Met 13:193
36. Conley R (1972) Infrared Spectrocopy, 2nd edn. Allyn and Bacon, Boston, MA, pp 196–198
37. Lee JY, Cui CQ, Su XH (1993) J Electroanal Chem 360: 177–187
38. Mav I, Zigon M, Sebenik A (1999) Synth Met 101:717–718
39. Fan J, Wan M, Zhu D (1998) J Polym Sci Part A: Polym Chem 36:3013–3019
40. Yue J, Epstein AJ (1990) J Am Chem Soc 112:2800–2801
41. Yue J, Wang ZH, Cromack KR, Epstein AJ, Macdimard AG (1991) J Am Chem Soc 113:2665–2671
42. Wei X, Wang Y, Long S, Bobeezko C, Epstein AJ (1996) J Am Chem Soc 118:2545–2555
43. Lapkowski M (1990) Synth Met 35:169–182
44. Bard AJ, Faulkner LR (1980) Electrochemical methods, fundamentals and applications. Wiley, New York, p 288 (Chapter 8)
45. Andrieux CP, Dumas-Bouchiat JM, Savéant JM (1982) J Electroanal Chem 131:1–35
46. Karabinas P, Jannakoudakis D (1984) J Electroanal Chem 160:159–167
47. Bard AJ, Faulkner LR (1980) Electrochemical methods, fundamentals and applications. Wiley, New York, p 143 (Chapter 5)
48. Galus Z (1976) Fundamentals of electrochemical analysis. Ellis Horwood, New York, p 313 (Chapter 10)